LASER INTERFEROMETER GRAVITATIONAL WAVE OBSERVATORY

- LIGO -

CALIFORNIA INSTITUTE OF TECHNOLOGY
MASSACHUSETTS INSTITUTE OF TECHNOLOGY

Document Type	LIGO-T010101-00-E	18 January 2002
Technical Note		

Analysis of the effects of long term correlations over long baselines over narrowband features in cross-correlation measurements

Albert Lazzarini, Andrea Vicerè, and Robert Schofield

California Institute of Technology
LIGO Laboratory, M/S 18-34
Pasadena, CA 91125
Phone: (626) 395-3064
Fax: (626) 304-9834
email: info@ligo.caltech.edu

Masachusetts Institute of Technology
LIGO Laboratory, M/S 16NW-145
Cambridge, MA 02139
Phone: (617) 253-4824
Fax: (617) 253-7014
email: info@ligo.mit.edu

www: http://www.ligo.caltech.edu

I. INTRODUCTION

During the LIGO engineering runs E3 - E6, Klimenko et al. studied the long-baseline correlations in the power line mains between the two LIGO observatory sites. It was observed that even for very long integration times the cross correlation persisted (see Fig. 1). At first, it might seem surprising that power lines separated by two thirds of a continent should exhibit any degree of phase correlation. The U.S. power grid is composed of two sectors that are separated by the Mississipi river into Eastern and Western sections, and the two LIGO interferometers, in Hanford (WA) and in Livingston (LA) belong respectively to the Western and Eastern sections. Upon further consideration, however, they cannot be completely independent because grid-wide constraints are imposed on the instantaneous and average deviation of the frequency from the reference frequency: the power grid phase stability is referenced to GPS. We have obtained information from the U.S. western grid authority that provides some insight on how frequency stabilization is implemented. More recently we also obtained data for the frequency corrections made at 1800s intervals over a one year period. Below we discuss how the grid frequency control mechanism manifests itself in the 60 Hz line shape and possibly in long-baseline cross correlations of mains signals.

II. U.S. POWER GRID FREQUENCY CONTROL STRATEGY

Let $\nu_{1,2}(t)$ be the instantaneous frequencies as seen at the two sites: they may be considered random variables, and analogously the phase at time t relative to epoch t_0 is given by

$$\phi_{1,2}(t) \equiv 2\pi \int_{t_0}^{t} \nu_{1,2}(t')\, dt' + \phi_{1,2}(t_0)\,; \tag{1}$$

we don't know in principle the distribution of ν and its consequent influence on ϕ, but we know that two kinds of constraints are imposed on them:

Average frequency: the frequency averaged over a sufficiently long time interval T is not allowed to differ more than a certain limit from the reference frequency ν_c (60 Hz in the United States):

$$\left| \int_{t_0}^{t_0+T} \nu_i(t)\, dt - \nu_c T \right| \leq \frac{\Delta\phi_{\max}}{2\pi}\,; \tag{2}$$

which is equivalent to limiting the accumulaiton of phase errors to values smaller than $\Delta\phi_{\max}$. Our present understanding[1] is that the phase is allowed to drift freely until

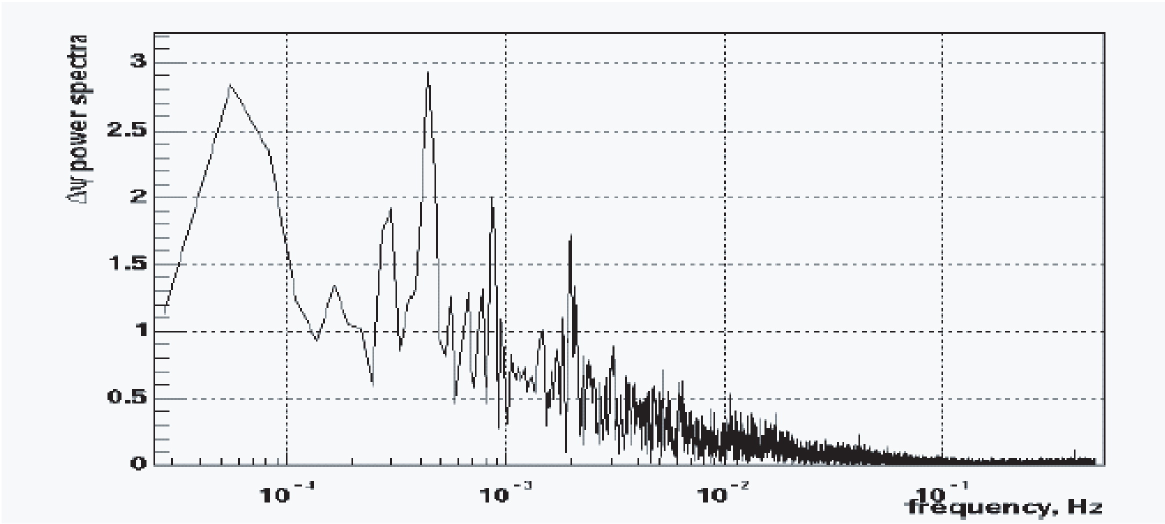

Figure 1: The spectral desnity of phase noise at 60 Hz as reported for the LIGO E3 engineering run by Klimenko et al. Graph taken from their LSC internal report (not numbered)

the constraint is approached. At this point, the frequency is changed in order to impose the constraint. Again, we currently understand that this manual regulation of the frequency is not needed more than once or twice per hour, hence the value of T at which the limit is reached is of order $\approx$ 1800sec. The value of $\Delta\phi_{\max}$ is fixed so that a clock using the line phase as a frquenct reference will never accumulate a time error greater than $\Delta t_{\max}$: this limit appears to be different for the Eastern and Western power grids[1]: in the West $\Delta t_{\max} = 2$s, while in the East $\Delta t_{\max} = 8$s and will be in the future increased to 10s. Correspondingly, we have

$$\Delta\phi_{\max} = (2\pi)\,\Delta t_{\max}\nu_c \tag{3}$$

and we have $\Delta\phi_{\max} \approx 754$ in the Western grid, $\Delta\phi_{\max} = 3770$ on the Eastern grid.

Instantaneous frequency deviation: the instantaneous value of $\nu_i\,(t) = \frac{d\phi_i(t)}{dt}$ is constrained within certain limits

$$\left|\nu_i\left(t\right)-\nu_c\right|\leq\Delta\nu_{\max} \tag{4}$$

with respect to the reference frequency ν_c. The current limit is[1] $\Delta\nu_{\max}=0.02$Hz.

III. DATA FROM THE U.S. WESTERN GRID

The data available consist of one year worth of time error signals, acquired on the Eastern power grid: they consist of the errors $\delta t\left[t\right]$ that result from using the phase of the power line as a clock, with respect to the reference phase

$$\phi_c\left(t\right)=2\pi\nu_c t \tag{5}$$

where ν_c=60Hz is the reference frequency on the grid. If $\phi\left(t\right)$ is the phase of the voltage actually delivered by the grid, then

$$\delta t\left(t\right)\equiv\frac{\phi\left(t\right)-\phi_c\left(t\right)}{2\pi\nu_c}; \tag{6}$$

these data are available sampled every 1800s, every half hour, and were taken in the period October 1st, 2000 – September 30, 2001.

We present in Fig. 2 a plot of the phase error

$$\delta\phi\left(t\right)\equiv 2\pi\nu_c\delta t\left(t\right) \tag{7}$$

and of the corresponding one-sided spectrum $S_\phi\left(f\right)$, normalized so as to have

$$E\left[\left(\delta\phi\left(t\right)-E\left[\delta\phi\left(t\right)\right]\right)^2\right]=\int_0^{f_{\mathrm{Nyquist}}}S_\phi\left(f\right)df. \tag{8}$$

The spectrum clearly shows peaks corresponding to 24 and 12 hours periodicity, as well as harmonics of these . There are also peaks corresponding to weekly and monthly periodicities.

We can define a "frequency shoft" by setting

$$\delta\nu\left(t\right)\equiv\frac{1}{2\pi}\frac{\delta\phi\left(t+\Delta t\right)-\delta\phi\left(t\right)}{\Delta t}: \tag{9}$$

the corresponding time series and spectrum are shown in Fig. 3 which displays also some spikes corresponding to sudden frequency variations, due to holes in the data.

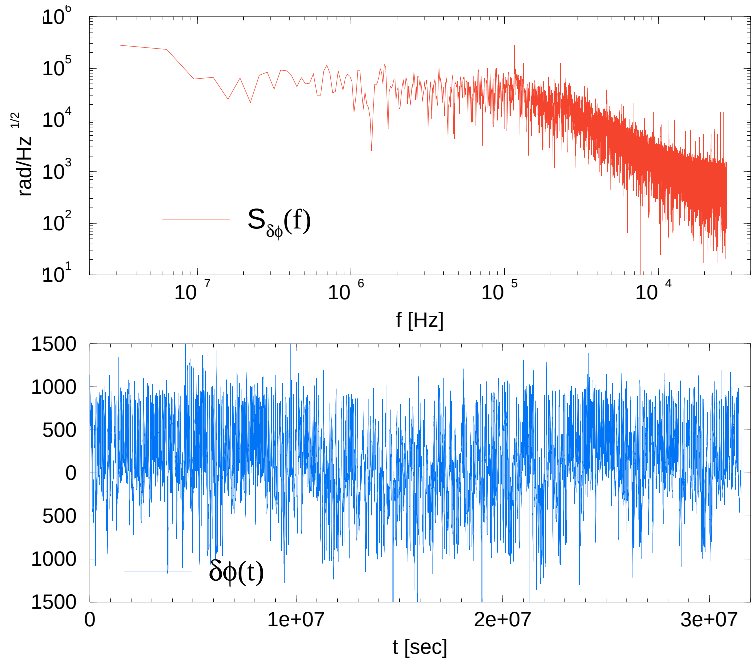

Figure 2: Time series and spectrum of the deviation $\delta\phi\,(t)$ of the voltage phase from the reference. There is a hint of seasonal dependence of the phase correction.

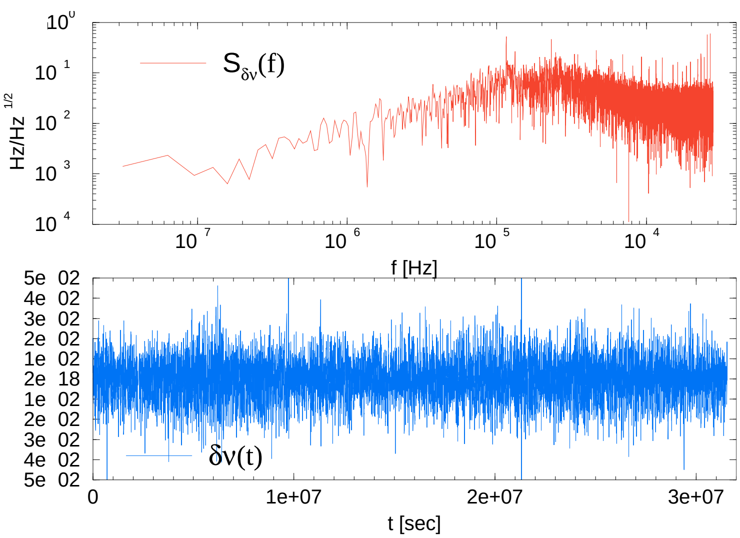

Figure 3: Time series and spectrum of the deviation $\delta\nu\,(t)$ of the voltage frequency from the reference ν_c.

A. Behavior of the noise on short timescales

It is useful to have a look at the data on shorter segments of time, as in Fig. 4, which displays 3.5 days worth of data. The trend of $\delta\phi$ suggests that the phase error grows roughly linearly in time over intervals of the order of a few hours, separated by abrupt changes in

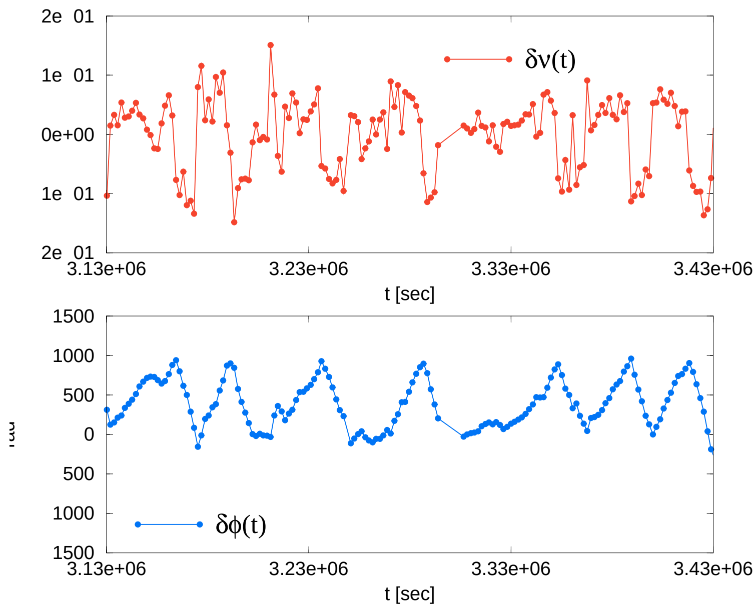

Figure 4: A zoom of $\delta\phi$ and $\delta\nu$ over a time range of approximately 3.5days.

direction. The slope changes from interval to interval, not just in sign but also in magnitude, as it is evidenced by the upper plot with the frequency: although a large frequency variation is evident also inside each interval, one can roughly divide the sample into segments of approximate constant frequency, separated by sudden jumps. This behaviour is particularly evident in the right side of the phase plot (and even more evident than in the frequency plot), and would suggest a bimodal behaviour for the frequency: to check for it, we plot in Fig. 5 several histograms of the data, obtained from 8 segments of 512 samples at the beginning of the dataset.

It is possible to see hints of bimodality in some of the histograms, but not very evident, and the two gaussians (if real) appear to have a variance comparable with the separation of their barycenters.

For a better understanding we attempted the following first-cut analysis: we divided the frequency data in blocks separated by the change of sign, we substituted in each block the value of the elements by the average value $\langle\delta\nu\rangle$ over the block, and then we recomputed a histogram of the resulting sequence. We did the same computing the standard deviation $\sigma_{\langle\delta\nu\rangle}$ on each block, and forming another sequence where each element on each block was substituted by the $\sigma_{\langle\delta\nu\rangle}$ value pertinent to that block.

The results are shown in Fig. 6: in particular the plot at left of the averages shows clearly

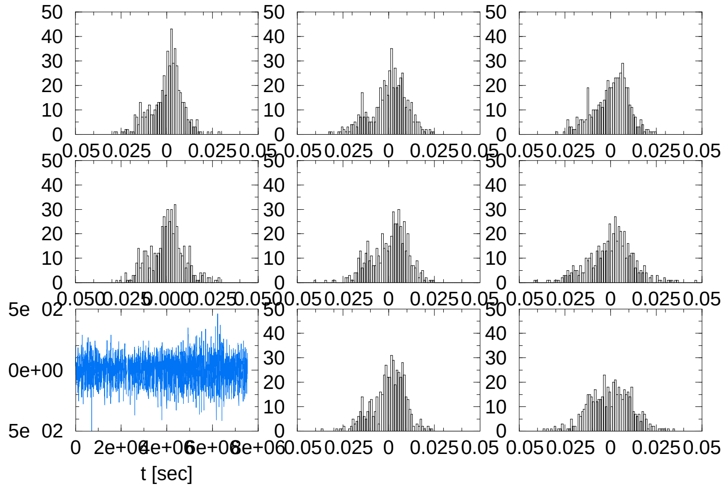

Figure 5: Histograms obtained from a few data segments of $\delta\nu$, each 512 data points long, taken at the beginning of the dataset.

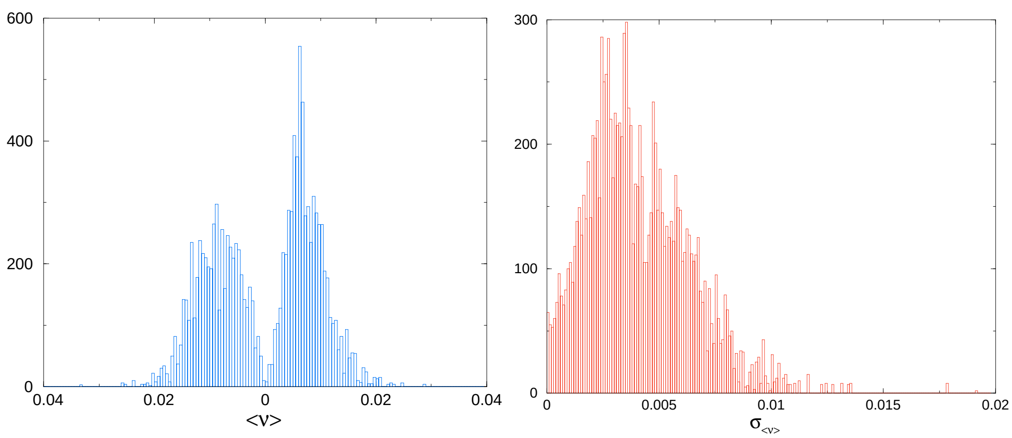

Figure 6: Left: the histogram of the averages computed over each block of ν data having the same sign, where each value of the averages contributes to the histogram a number of times equal to the length of the block. Right: the same histogram for the standard deviations, computed on the same data and the same blocks.

a clustering, while in the plot at right the histogram of the standard deviations displays a rather wide distribution.

One may surmise that the variances on each block depend on the average value: to test for this we plot in Fig. 7 the standard deviations $\sigma_{\langle\delta\nu\rangle}$ versus the averages $\langle\delta\nu\rangle$.

The plot clearly shows that there is a correlation, which looks vaguely linear: a simple fit results in

$$\sigma_{\langle\delta\nu\rangle} \sim 0.46983(5)\,|\langle\delta\nu\rangle|\,. \tag{10}$$

Assuming that there is indeed a relation between $\langle\delta\nu\rangle$ and $\sigma_{\langle\delta\nu\rangle}$, and that the spread is

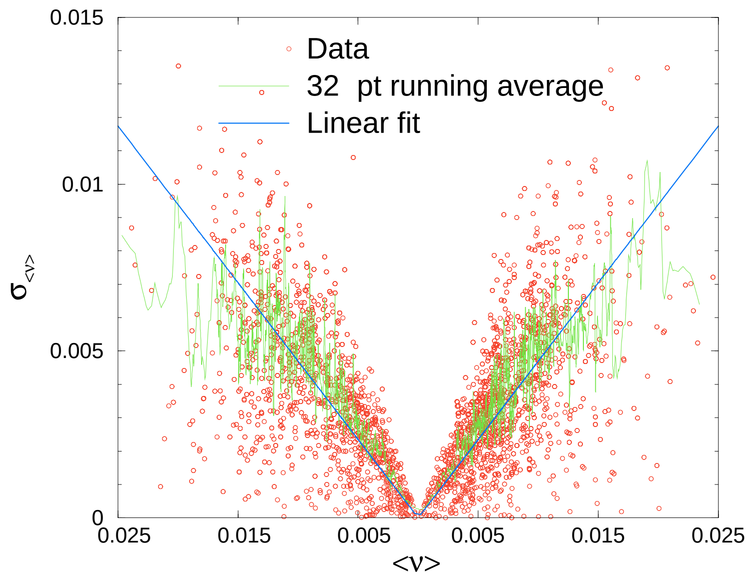

Figure 7: The standard deviations $\sigma_{\langle\delta\nu\rangle}$ calculated on each block versus the averages $\langle\delta\nu\rangle$: a correlation is apparent. Also shown is a 64-pt moving average of the $\sigma_{\langle\delta\nu\rangle}$ values: the cusp in zero is an artefact of the averaging procedure.

statistical noise, we visually improve the estimation of $\sigma_{\langle\delta\nu\rangle}$by performing a 64-pt running average over close values of $\langle\delta\nu\rangle$: the resulting curve is superimposed to the plot and is in good agreement with the fit.

The whole analysis is clearly biased by the way we divide the $\delta\nu$ data in blocks, simply looking at sign changes: yet it seems to give a reasonable description of the process, and we can argue that on each block we have a frequency noise of the form

$$\delta\nu_i \sim \langle\delta\nu\rangle\,(1 + s\,\xi_i) \tag{11}$$

where $\langle\delta\nu\rangle$ is a random number, constant on each block, with a bimodal distribution as in the left of Fig. 6, while $s \simeq 0.47$ is the scale relating $\sigma_{\langle\delta\nu\rangle}$ and $\langle\delta\nu\rangle$ in Eq. 10; ξ_i is a gaussian white noise with unit variance.

We want now to understand the statistics of the "frequency hop" events which lead to jumps in $\langle\delta\nu\rangle$. are subject to a Poisson distribution, and to test for this we report in Fig. 8 the distribution of the lengths of the blocks, or in other words of the interval between jumps.

If the jumps are Poisson points, then the distribution of the intervals Δt should be

$$p\,(\Delta t) = \lambda^2 \Delta t\, e^{-\lambda\Delta t}; \tag{12}$$

there is some hint of such a distribution if one disregards the first two bings of the histogram:

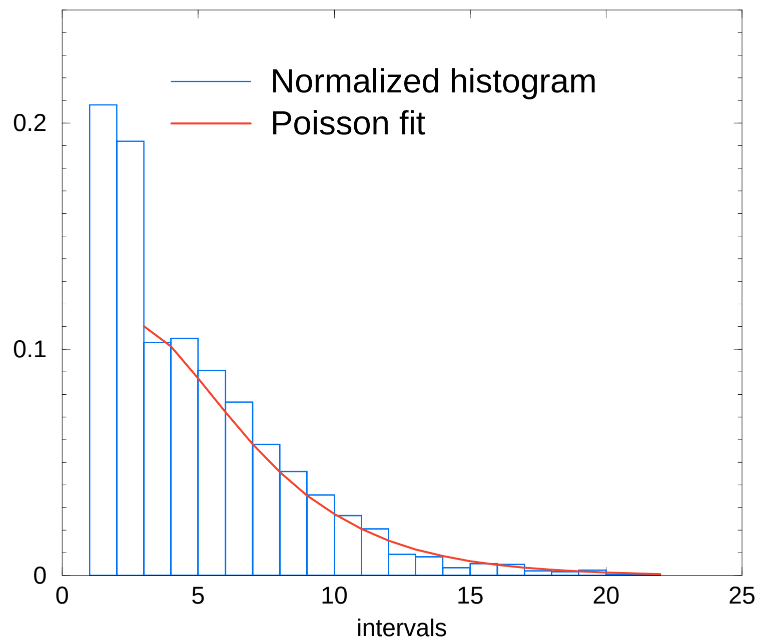

Figure 8: The distribution of the intervals between sign changes of $\langle \delta\nu \rangle$. A Poisson distribution is superimposed, obtained dropping the first two points of the histogram, pretending that they are an artefact due to the way the data are separated in blocks.

fitting one obtains a value of $\lambda \sim 0.37$, corresponding to an average interval

$$\langle \Delta t \rangle = \frac{2}{\lambda} \times 1800 \simeq 9730\text{sec} \tag{13}$$

between events. The reason for dropping the first two bins is that one can suspect that the procedure used in separating the intervals (just by the sign of $\delta\nu$) is imperfect, and that intervals having an average $\langle \delta\nu \rangle$ close to zero may have been artificially split in two, artificially increasing the frequency of short intervals. Of course this adversely affects also the frequency of long ones, and one may surmise that λ has been overstimated.

B. The deduced 60 Hz lineshape

The sampling rate of 1800 sec gives no direct access to the frequency range of the 60Hz line and its harmonics: it is however possible to gain some insight on the lineshape, by treating $\delta\phi$ as a Gaussian variable with the spectrum given in Fig. 2. For definitess let us consider the time series

$$n(t) \equiv \cos\left(2\pi\nu_c t + \delta\phi(t)\right) : \tag{14}$$

we are interested in estimate its spectrum, which deviates from a δ function at ν_c because of the noisy $\delta\phi$. We first rewrite

$$n(t) = \frac{1}{2}\left(z(t) + z^*(t)\right) \tag{15}$$

where

$$z(t) \equiv e^{i2\pi\nu_c t + \delta\phi(t)} : \tag{16}$$

the correlation matrix is

$$\begin{aligned} R_n(t+\tau\, t) &\equiv E\left[n(t+\tau)\, n(t)\right] \\ &= \frac{1}{2}\Re\left(R_{zz}(t+\tau, t) + R_{zz^*}(t+\tau, t)\right) \end{aligned} \tag{17}$$

and

$$\begin{aligned} R_{zz^*}(t+\tau, t) &= e^{i2\pi\nu_c\tau} E\left[e^{i(\delta\phi(t+\tau)-\delta\phi(t))}\right] \\ &= e^{i2\pi\nu_c\tau - \frac{1}{2}E\left[(\delta\phi(t+\tau)-\delta\phi(t))^2\right]} \\ &= e^{i2\pi\nu_c\tau - R_{\delta\phi}(0) + R_{\delta\phi}(\tau)} \end{aligned} \tag{18}$$

while

$$\begin{aligned} R_{zz}(t+\tau, t) &= e^{i2\pi\nu_c(2t+\tau)} E\left[e^{i(\delta\phi(t+\tau)+\delta\phi(t))}\right] \\ \\ &= e^{i2\pi\nu_c(2t+\tau) - R_{\delta\phi}(0) - R_{\delta\phi}(\tau)}, \end{aligned} \tag{19}$$

hence

$$R_n(t+\tau, t) = \frac{1}{2} e^{-R_{\delta\phi}(0)} \Re\left[e^{i2\pi\nu_c(2t+\tau) - R_{\delta\phi}(\tau)} + e^{i2\pi\nu_c\tau + R_{\delta\phi}(\tau)}\right] : \tag{20}$$

averaging over t we can define

$$\begin{aligned} R_n(\tau) &= \frac{1}{T}\int_0^T R_n(t+\tau, t)\, dt \\ &= \frac{1}{2}\cos(2\pi\nu_c\tau)\, e^{-R_{\delta\phi}(0) + R_{\delta\phi}(\tau)} + O\left(T^{-1}\right). \end{aligned} \tag{21}$$

The one-sided noise spectrum follows:

$$\begin{aligned} S_n(\omega) &= 2\int_{-\infty}^{+\infty} R_n(|\tau|)\, e^{-i\omega\tau} d\tau \\ &= \frac{1}{2} e^{-R_{\delta\phi}(0)} \int_{-\infty}^{+\infty} \left[e^{i(2\pi\nu_c - \omega)\tau + R_{\delta\phi}(|\tau|)} + e^{-i(2\pi\nu_c + \omega)\tau + R_{\delta\phi}(|\tau|)}\right] d\tau \\ &= e^{-R_{\delta\phi}(0)} \Re \int_0^{+\infty} \left[e^{i(2\pi\nu_c - \omega)\tau + R_{\delta\phi}(\tau)} + e^{-i(2\pi\nu_c + \omega)\tau + R_{\delta\phi}(\tau)}\right] d\tau \end{aligned}$$

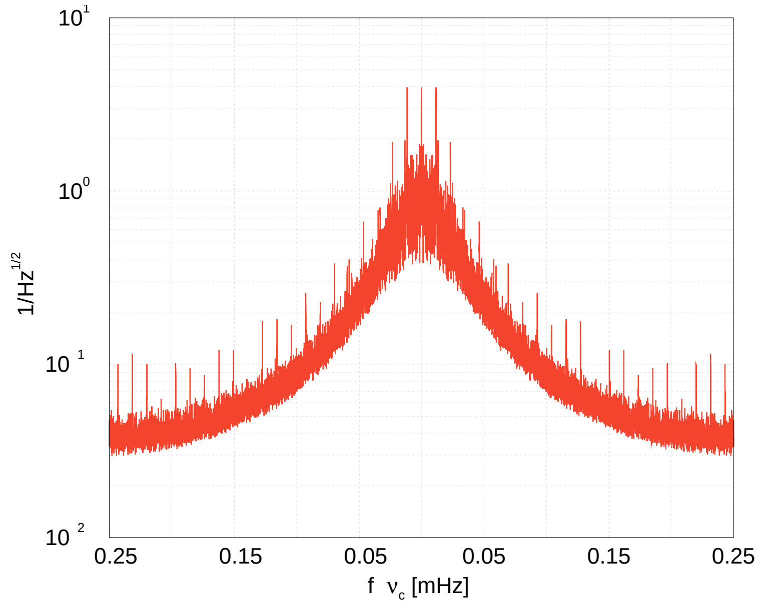

Figure 9: The lineshape due to fluctuations of the phase, as deduced from the data on $\delta\phi$, plotted as a function of the difference $f - \nu_c$ from the $\nu_c = 60$Hz reference frequency; notice also the scale of the abscissa in mHz.

which can be written in the form

$$S_n(\omega) = L_n(\omega - 2\pi\nu_c) + L_n(\omega + 2\pi\nu_c) \tag{22}$$

where we have introduced the lineshape

$$L_n(\Delta\omega) \equiv \Re \int_0^\infty e^{i\Delta\omega\tau} e^{R_{\delta\phi}(\tau) - R_{\delta\phi}(0)} d\tau. \tag{23}$$

This formula merely indicates that a knowledge of $R_{\delta\phi}(\tau)$ for large τ, or equivalently of $S_{\delta\phi}(\Delta\omega)$ for small $\Delta\omega$, allows to determine the lineshape for small $\Delta\omega$: the result is shown in Fig. 9

A sideband structure, due to the periodicities in the $\delta\phi$ data, is evident, along with a continuum structure which reminds of the random walk performed by the frequency during the "free fall" intervals between inversions.

All this is interesting but does not tell us much about possible wideband effects[1] of these line fluctuations. In order to say more about them, we need to make an ansatz on the phase (and frequency) fluctuations over shorter time scales.

[1] Namely, outside the 0.25mHz band we are restricted to by the sampling frequency of the $\delta\phi$ data.

IV. MODEL FOR THE PHASE NOISE

As a first step, a simple matlab model was built that implements the control laws outlined in Section I. A schematic block diagram for the *simulink* model is shown in Fig. 10 and the resultant cross-spectrum showing structure on the flanks fo the mains line is also shown in the figure.

We consider the stochastic processes $\frac{\phi_{1,2}}{2\pi}$ to be biased random walks, each of them with the constraint that the average speed over time interval T

$$\overline{\nu}(t) \equiv \frac{\phi(t+T)-\phi(t)}{2\pi T} \in \nu_c \left[1-\frac{\Delta t_{\max}}{T}, 1+\frac{\Delta t_{\max}}{T}\right] \tag{24}$$

is limited to a range around ν_c, whose width is proportional to $2\frac{\Delta t_{\max}}{T}$; and with the constraint on the instantaneous speed

$$\nu(t) \in \nu_c \left[1-\frac{\Delta\nu_{\max}}{\nu_c},\ 1+\frac{\Delta\nu_{\max}}{\nu_c}\right] \tag{25}$$

to lie in the interval specified in Eq. (4).

It is advantageous to change variables in order to have zero-mean: let

$$\omega_c \equiv 2\pi\nu_c \tag{26}$$

and

$$\psi(t) \equiv \phi(t) - \omega_c t \tag{27}$$

the constraints for $\boldsymbol{\psi}_i$ would correspondingly become

$$|\psi(t+T)-\psi(t)| \ \leq\ \Delta\phi_{\max}\,\forall t, T \tag{28a}$$

$$\left|\frac{d\psi(t)}{dt}\right| \ \leq\ 2\pi\Delta\nu_{\max}\,\forall t. \tag{28b}$$

It is important to notice that the constraint on the phase, Eq. 28a can also be rewritten as

$$|\psi(t_1)-\psi(t_2)| \leq \Delta\phi_{\max}\,\forall t_1, t_2 \tag{29}$$

which seems obvious but is illuminating, because it is equivalent to say, setting $t_2 = 0$, that

$$|\psi(t)| \leq \frac{\Delta\phi_{\max}}{2}\,\forall t. \tag{30}$$

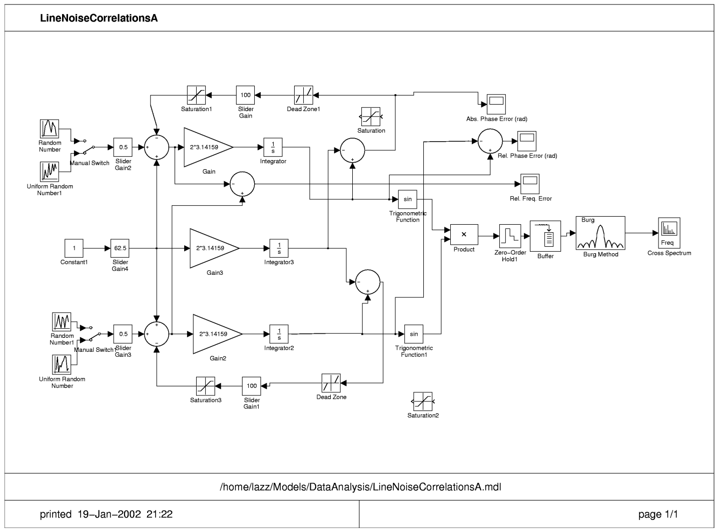

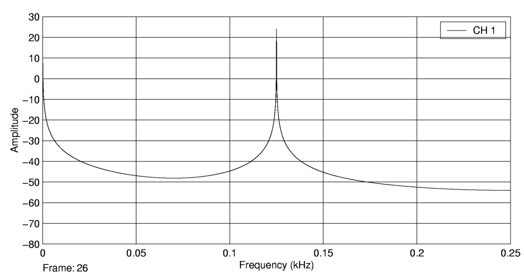

Figure 10: Schematic of a Matlab model that implements the control laws used the the U.S. grid authority which were discussed in Section I. The frequency correction can give rise to sideband structure of the power main 60 Hz line.

It should be clear that several different models for $\boldsymbol{\psi} i$ can be compatible with the constraints in Eq. (28): the detailed form shall depend on the control strategy adopted by the power plants. In particular, it appears that most control systems are implemented with a "dead band": no control strategy is applied until the limits are reached. This suggests that the time evolution of the frequency is dominated indeed by a random walk, driven by the stochastic variation of the load on the grid.

A. Simplified model for the power generation

A very simple model for the time evolution of the frequency ν (we shall drop the suffix specifying the power grid) can be represented by a time varying viscosity, balanced in the average by the power of the generators in order to keep the frequency at ν_c: the differential equation for $\nu(t)$ is therefore

$$\dot{\nu}(t) + \beta_L(t)\,\nu(t) = \beta_G(t)\,\nu_c \tag{31}$$

where $\beta_L(t)$ represents the load on the grid, while $\beta_G(t)\,\nu_c$ represents the "force" applied by the generators: if $\beta_G(t) = \beta_L(t)$ this equation has the solution $\nu(t) = \nu_c$.

The detailed dependence of β_G on time depends on the control strategy: if the power plants adopt a "dead band" control strategy, its value shall be constant until the constraints are reached; in this case we can assume that during the "free fall" interval $\beta_G = E[\beta_L(t)]$, in other words that the power applied matches the average load.

In general we split

$$\beta_L(t) = \beta_G(t) + \delta\beta(t) \tag{32}$$

into a compoment $\beta_G(t)$which exhibits only slow variations in time, as appropriate to a control band resticted to the low frequency portion of the spectrum, and a stochastic process $\boldsymbol{\delta\beta}$ that displays also rapid variations, and whose spectrum is therefore uniform.

Correspondingly, we can assume that $\nu(t) = \nu_c + \delta\nu(t)$; substituting into Eq. (31) and dropping terms quadratic in the deviations from the average, we obtain

$$\delta\dot{\nu}(t) + \beta_G(t)\,\delta\nu(t) + \delta\beta(t)\,\nu_c = 0 \tag{33}$$

a equation which can be directly integrated. Referring to initial conditions at epoch t_0 we obtain

$$\delta\nu(t) = \delta\nu(t_0) - \nu_c e^{-\int_{t_0}^{t}\beta_G(\tau)d\tau}\int_{t_0}^{t} e^{\int_{t_0}^{\tau}\beta_G(\tau')d\tau'}\delta\gamma(\tau)\,d\tau; \tag{34}$$

without loss of generality we shall set from now on $\delta\nu(t_0) = 0$. The spectral content of the stochastic process $\boldsymbol{\delta\nu}$ depends on the detailed form of $\beta_G(t)$ and on the spectrum of the process $\boldsymbol{\delta\gamma}$. For the latter, we can assume that it is gaussian: therefore it can be expressed as a Riemann-Stiltjes integral

$$\delta\beta(t) = \int_{-\infty}^{+\infty} e^{i\omega t} \frac{d\tilde{\beta}(\omega)}{2\pi} \tag{35}$$

and the random increments $d\tilde{\beta}(\omega)$ are uncorrelated

$$E\left[\frac{d\tilde{\beta}(\omega)}{2\pi}\frac{d\tilde{\beta}^*(\omega')}{2\pi}\right] = \delta(\omega - \omega') S_\beta(\omega) \frac{d\omega}{2\pi}; \tag{36}$$

the symbol $E[\ldots]$ denotes the operation of *ensemble* averaging and $S_\beta(\omega)$ is two sided spectrum of the process $\boldsymbol{\delta\beta}$.

For simplicity we shall however assume that $S_\beta(\omega)$ is white and therefore the variables $\delta\beta(t)$, which are the instantaneous variation of the grid load, are δ-correlated

$$E[\delta\beta(t)\,\delta\beta(t')] = \sigma_\beta^2 \delta(t - t') \tag{37}$$

while

$$E[\delta\nu(t)\,\delta\nu(t')] = \sigma_\beta^2 \nu_c^2 \int_{t_0}^{\min(t,t')} e^{-\int_\tau^t \beta_G(\tau')d\tau' - \int_\tau^{t'} \beta_G(\tau')d\tau'} d\tau \tag{38}$$

which in general may not depend only on the difference $t - t'$.

B. Constant average load case

We should now specify a form for the slow evolution of the load on the grid, β_G: if we can assume $\beta_G(t) = \bar{\beta}_G$ constant, then our problem reduces itself to the classical Orstein-Uhlenbeck process[2, pag. 349] with the equation of motion

$$\delta\dot{\nu}(t) + \bar{\beta}_G \delta\nu(t) = -\delta\beta(t)\,\nu_c \tag{39}$$

and we have simply

$$\delta\nu(t) = -\nu_c \int_{t_0}^{t} e^{-\bar{\beta}_G(t-\tau)} \delta\beta(\tau)\,d\tau\,; \tag{40}$$

consequently

$$E[\delta\nu(t)\,\delta\nu(t')] = \frac{\sigma_\beta^2 \nu_c^2}{2\bar{\beta}_G}\left(e^{-\bar{\beta}_G|t-t'|} - e^{-\bar{\beta}_G(t+t'-2t_0)}\right) \tag{41}$$

and choosing $t_0 \ll t, t'$ we can neglect the second term: it results an exponential correlation

$$E\left[\delta\nu\left(t\right)\delta\nu\left(t'\right)\right] \approx \sigma_\nu^2 e^{-\frac{|t-t'|}{\tau_\nu}}, \tag{42}$$

where we set $\sigma_\nu^2 \equiv \frac{\sigma_\beta^2 \nu_c^2}{2\bar{\beta}_G}$, $\tau_\nu = \left(\bar{\beta}_G\right)^{-1}$; the correlation depends only on the difference of times, hence $\boldsymbol{\delta\nu}$ is a wide-sense stationary process, and

$$S_\nu\left(\omega\right) = \frac{2\sigma_\nu^2\tau_\nu}{1+\left(\omega\tau_\nu\right)^2} \tag{43}$$

is the expression of the two-sided spectrum of ν, which is *lorenzian*.

C. A more refined control model

The control model considered above reacts to the instantaneous deviations $\delta\nu$ from the reference frequency ν_c: a more realistic model would be one in which the control reacts on the average variations of the frequency over a time scale T_C. A simple modification of the model in Eq. (33) which implements this control law is

$$\delta\dot{\nu}\left(t\right) + \frac{\bar{\beta}}{T_c}\int_{t-T_c}^{t}\delta\nu\left(\tau\right)d\tau + \delta\beta\left(t\right)\nu_c = 0 \tag{44}$$

which leads to the relation

$$\frac{d\tilde{\nu}\left(\omega\right)}{2\pi} = \frac{\nu_c}{i\omega + \frac{2\bar{\beta}}{\omega T_c}e^{-i\omega T_c/2}\sin\left(\frac{\omega T_c}{2}\right)}\frac{d\tilde{\beta}\left(\omega\right)}{2\pi} \tag{45}$$

between the uncorrelated increments in the spectral representation of the random processes $\boldsymbol{\delta\nu}, \boldsymbol{\delta\beta}$. It follows the relation among the spectra

$$S_\nu\left(\omega\right) = \frac{\nu_c^2}{\omega^2 + \frac{4\bar{\beta}}{T_c}\left(\frac{\bar{\beta}}{\omega^2 T_c} - 1\right)\left[\sin\left(\frac{\omega T_c}{2}\right)\right]^2}S_\beta\left(\omega\right); \tag{46}$$

for small T_c one obtains

$$S_\nu\left(\omega\right) \approx \left[\frac{\nu_c^2}{\omega^4 T_c^2\left(\frac{T_c\bar{\beta}}{12} + \frac{T_c^2\bar{\beta}^2}{360}\right) + \omega^2\left(1 - T_c\bar{\beta} - \frac{T_c^2\bar{\beta}^2}{12}\right) + \bar{\beta}^2}\right]S_\beta\left(\omega\right). \tag{47}$$

Up to T_c^2 order the form of the gain (the expression in square parentheses) is *lorenzian* as in the previous case, leading to a exponential correlation with a modified time constant

$$\tau_\nu = \frac{\sqrt{1 - T_c\bar{\beta} - \frac{T_c^2\bar{\beta}^2}{12}}}{\bar{\beta}}. \tag{48}$$

If we instead retain up to T_c^4 order, the functional form of the gain changes, and for $T_c\bar{\beta} \geq 1$ it leads to a oscillating correlation function.

Given a expression for the spectrum

$$P(\delta\nu) \propto \exp\left[-\frac{1}{2}\int_{-\infty}^{+\infty}\frac{|\delta\tilde{\nu}(\omega)|^2}{S_\nu(\omega)}\frac{d\omega}{2\pi}\right] \tag{49}$$

is the explicit expression for the probability distribution of the process $\boldsymbol{\delta\nu}$.

D. The phase as a non-stationary random process

The reduced phase ψ referred to epoch t_0 is by definition given by

$$\psi(t) = 2\pi\int_{t_0}^{t}\delta\nu(\tau)\,d\tau + \psi(t_0) \tag{50}$$

where also $\psi(t_0)$ is in general a random variable. The process $\boldsymbol{\psi}$ is random with stationary increments[5, 6]: the statistical properties of this class of stochastic processes are completely determined by the structure function[2]

$$c_\psi(t,u) \equiv E\left[(\psi(t)-\psi(u))^2\right]; \tag{51}$$

for instance, if one is interested in the correlation of increments referred to the same origin u, it is easily seen that

$$E\left[(\psi(t)-\psi(u))(\psi(t')-\psi(u))\right] = \frac{1}{2}\left[c_\psi(t,u)+c_\psi(t',u)-c_\psi(t,t')\right] \tag{52}$$

a identity independent on the explicit expression of ψ. In our case, we know the statistics of the process $\boldsymbol{\delta\nu}$, and it is immediate to compute the structure function:

$$\begin{aligned} c_\psi(t,u) &= (2\pi)^2\int_u^t d\tau\int_u^t d\tau' E\left[\delta\nu(\tau)\,\delta\nu(\tau')\right] \\ &= (2\pi)^2\int_0^{t-u} d\tau\int_0^{t-u} d\tau'\rho_\nu(\tau-\tau') \\ &= (2\pi)^2\int_{-(t-u)}^{t-u}(t-u-|\tau|)\,\rho_\nu(\tau)\,d\tau \end{aligned}$$

[2] In the specialized literature the structure functions are usually expressed with a D symbol, which we prefer to reserve for the diffusion constant. Notice also that for complex processes $\boldsymbol{\xi}$ it is instead necessary to consider the more general expression

$$c_\xi(t;u,v) \equiv E\left[(\xi(u)-\xi(t))(\xi(v)-\xi(t))^*\right]$$

which depends on three variables.

which depends only on the difference $t-u$, and shall be called $c_\psi(t-u)$ from now on. The linear growth of the variance

$$E\left[(\psi(t)-\psi(t_0))^2\right]=(2\pi)^2(t-t_0)\int_{-(t-t_0)}^{t-t_0}\left(1-\frac{|\tau'|}{t-t_0}\right)\rho_\nu(\tau')\,d\tau' \tag{53}$$

with the distance $t-t_0$ from the origin exposes the non-stationarity of the $\boldsymbol{\psi}$ process, which behaves like a diffusion. When in particular ρ_ν is exponential we obtain

$$\begin{aligned} c_\psi(T) &= (2\pi)^2\sigma_\nu^2\int_{-T}^{T}(T-|\tau|)\,\sigma_\nu^2 e^{-\frac{|\tau|}{\tau_\nu}}d\tau \\ &= \alpha_\nu\left[\frac{T}{\tau_\nu}-\left(1-e^{-\frac{T}{\tau_\nu}}\right)\right] \end{aligned} \tag{54}$$

where we have introduced the adimensional constant

$$\alpha_\nu\equiv 2\,(2\pi)^2\,\sigma_\nu^2\tau_\nu^2\,. \tag{55}$$

If $T\gg\tau_\nu$ we can neglect the exponential term, obtaining

$$c_\psi(T)=E\left[(\psi(t+T)-\psi(t))^2\right]\approx\alpha_\nu\frac{T}{\tau_\nu}\equiv 2D_\psi^2 T \tag{56}$$

where we have introduced

$$D_\psi=(2\pi)\,\sigma_\nu\sqrt{\tau_\nu} \tag{57}$$

for *large* T the process $\boldsymbol{\psi}$ behaves as a diffusion with *diffusion constant* D_ψ: but T must be very large, because we shall see immediately that τ_ν is in our case not small.

Another interesting quantity is the variance of the process $\psi(t)$ itself

$$\sigma_\psi^2(t)\equiv E\left[(\psi(t))^2\right] \tag{58}$$

and we expect it to be a growing function of time. We are interested in computing the difference $\sigma_\psi^2(t)-\sigma_\psi^2(t_0)$: notice the identity

$$\begin{aligned} E\left[(\psi(t))^2\right] &= E\left[((\psi(t)-\psi(t_0))+\psi(t_0))^2\right] \\ &= c_\psi(t-t_0)+2E\left[(\psi(t)-\psi(t_0)\,\psi(t_0))\right]+E\left[(\psi(t_0))^2\right] \end{aligned} \tag{59}$$

and we observe also that

$$\begin{aligned} 2E\left[(\psi(t)-\psi(t_0))\,\psi(t_0)\right] &= 2E\left[(\psi(t)-\psi(t_0))\,(\psi(t_0)-\psi(t_0-T)+\psi(t_0-T))\right] \\ &= -\left[c_\psi(t-t_0)+c_\psi(T)-c_\psi(t-t_0+T)\right] \\ &\quad +2E\left[\left(\int_{t_0}^{t}\delta\nu(\tau)\,d\tau\right)\psi(t_0-T)\right]; \end{aligned} \tag{60}$$

if the process $\delta\nu(t)$ has a finite memory (in our case, $O(\tau_\nu)$) we can assume that the last term is zero for T large enough. Hence we have

$$\begin{aligned} \sigma_\psi^2(t) - \sigma_\psi^2(t_0) &= \lim_{T\to\infty} \left[c_\psi(t - t_0 + T) - c_\psi(T)\right] \\ &= \alpha_\nu \frac{t - t_0}{\tau_\nu} \end{aligned} \tag{61}$$

which exposes perhaps more clearly that the process behaves as a diffusion.

E. Imposing the constraints of the grid on the model

We are now in position to impose the constraints on the instantaneous and average frequency, at least approximately. We recall that in Eqs. (28) we had set limits on $|\delta\nu(t)|$ and on $\frac{1}{T}|\psi(t+T) - \psi(t)|$; we trade these hard limits with soft limits on the variance, corrected by appropriate factors to partially account for substituting averages over a interval with Gaussian averages

$$E\left[(\delta\nu(t))^2\right] = \sigma_\nu^2 \leq \frac{1}{3} \times \Delta\nu_{\max}^2 = 133.3 \times 10^{-6}\,\mathrm{Hz}^2 \tag{62a}$$

$$E\left[\left(\psi\left(t + \frac{1}{2}T_{1\mathrm{d}}\right) - \psi(t)\right)^2\right] = (2\pi)^2\, 2\sigma_\nu^2 \tau_\nu \left(\frac{1}{2} 86400 - \tau_\nu - e^{-\frac{86400}{2\tau_\nu}}\right) \leq \frac{1}{3} \times \Delta\phi_{\max}^2 \tag{62b}$$

where we have assumed the phase average is taken over half a day; taking the inequalities as equalities we obtain

$$\sigma_\nu \approx 11.5 \times 10^{-3}\mathrm{Hz} \tag{63a}$$

$$\tau_\nu \approx (420,\ 17500)\ \mathrm{sec}\,. \tag{63b}$$

where the two values for τ_ν refer respectively to the Western and Eastern grid. Consequently the estimate of the diffusion constant for the process $\boldsymbol{\psi}$is

$$D_\psi \approx (1.5,\ 9.6)\,\sqrt{\mathrm{Hz}}; \tag{64}$$

however T must be much larger then τ_ν in order for the approximation in Eq. (56) to be valid, particularly for the Eastern grid where τ_ν is rather large. The conditions that we have imposed should be interpreted as characteristics of the random processes which ensure that the frequency error does not exceed significantly the 20mHz limit in Eq. (28b), and that the 120 cycles constraint on the phase in Eq. (28a) is exceeded twice a day.

The conditions in Eqs. (62) are sufficient to specify the characteristics of the diffusion process, but do not implement the control strategy which is known to operate twice a day in order to constrain the phase error $\psi(t)$.

It is useful to introduce the transition probability $P(\psi, t|\psi_0, t_0)$ of observing a value ψ at time t, given that it was ψ_0 at time t_0: we know that $\psi - \psi_0$ is a Gaussian variable, and from the results of the previous sections we deduce that

$$P(\psi, t|\psi_0, t_0) = \frac{1}{\sqrt{(2\pi) c_\psi (t - t_0)}} e^{-\frac{1}{2}\frac{(\psi-\psi_0)^2}{c_\psi(t-t_0)}} \tag{65}$$

where the variance is expressed by the structure function $c_\psi(\tau)$. It is immediate to show that the process $\boldsymbol{\psi}$ is *not* Markovian, because

$$P(\psi, t|\psi_0, t_0) \neq \int_{-\infty}^{+\infty} P(\psi\, t|\psi_1, t_1) P(\psi_1, t|\psi_0, t_0)$$

as a consequence of

$$c_\psi(t - t_0) \neq c_\psi(t - t_1) + c_\psi(t_1 - t_0) \ . \tag{66}$$

The transition probability is the solution of the Fokker-Planck *diffusion* equation

$$\frac{\partial P}{\partial t} - \frac{1}{2} c'_\psi(t - t_0) \frac{\partial^2 P}{\partial \psi^2} = 0 \tag{67}$$

with the boundary condition $P(\psi, t|\psi_0, t) = \delta(\psi - \psi_0)$. We implement the control strategy by imposing that no probability current flows outside of the interval $[\psi_0 - \Delta\phi_{\max}, \psi_0 + \Delta\phi_{\max}]$: we ask therefore that

$$\frac{\partial P(\psi\, t|\psi_0, t_0)}{\partial \psi}|_{\psi=\psi_0\pm\Delta\phi_{\max}} = 0 \tag{68}$$

and we solve the equation expanding in Fourier series

$$P(\psi, t|\psi_0, t_0) = \sum_{k=0}^{\infty} \tilde{P}_k(t - t_0) \cos\left(\frac{\pi k(\psi - \psi_0)}{\Delta\phi_{\max}}\right) \tag{69}$$

obtaining

$$\frac{\partial \tilde{P}_k}{\partial t} + \frac{1}{2} c'_\psi(t - t_0) \left(\frac{\pi k}{\Delta\phi_{\max}}\right)^2 \tilde{P}_k = 0, \tag{70}$$

hence the solution normalized on the $[\psi_0 - \Delta\phi_{\max}, \psi_0 + \Delta\phi_{\max}]$ interval is

$$P(\psi, t|\psi_0, t_0) = \frac{1}{2\Delta\phi_{\max}} \sum_{k=-\infty}^{\infty} e^{-\frac{1}{2}c_\psi(t-t_0)\left(\frac{\pi k}{\Delta\phi_{\max}}\right)^2 + i\pi k\frac{(\psi-\psi_0)}{\Delta\phi_{\max}}}; \tag{71}$$

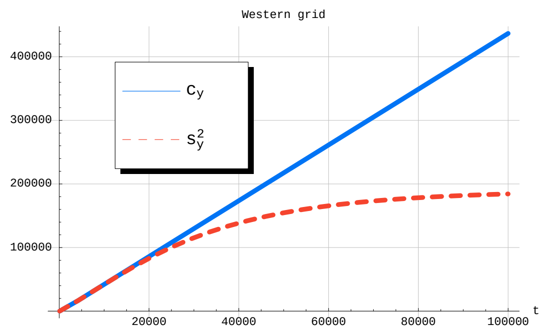

Figure 11: The comparison between the exact form of the structure function $E\left[\left(\psi\left(t\right)-\psi\left(t_0\right)^2\right]$ for the process $\boldsymbol{\psi}$ and the approximation $c_\psi\left(t-t_0\right)$. The plot at left is obtained with the values appropriate for the Western grid, while the plot at right is appropriate for the Eastern grid

it should be clear that for $c_\psi\left(t-t_0\right) \ll \Delta\phi_{\max}$ the sum can be replaced by a integral and converges to the expression in Eq. 65.

For arbitrary times one has that the variance is

$$
\begin{aligned}
E\left[\left(\psi\left(t\right)-\psi_0\left(t_0\right)\right)^2\right] &= \int_{-\Delta\phi_{\max}}^{+\Delta\phi_{\max}} \left(\psi\right)^2 P(\psi, t-t_0) d\psi \\
&= \frac{\Delta\phi_{\max}^2}{3}\left[1+\frac{12}{\pi^2}\sum_{k=1}^{\infty}\frac{(-1)^k}{k^2} e^{-\frac{1}{2}c_\psi(t-t_0)\left(\frac{\pi k}{\Delta\phi_{\max}}\right)^2}\right];
\end{aligned}
\tag{72}
$$

for $t=t_0$ one has $c_\psi\left(0\right)=0$ and the variance is zero as expected. For large $t-t_0$ instead $c_\psi \to \infty$, and the series goes to zero, hence

$$
\lim_{t-t_0\to\infty} E\left[\left(\psi\left(t\right)-\psi\left(t_0\right)\right)^2\right] = \frac{\Delta\phi^2}{3} \tag{73}
$$

while for small $t-t_0$ converges to $c_\psi\left(t-t_0\right)$.

We were unable to find a closed form for the variance (the structure function) $E\left[\left(\psi\left(t\right)-\psi\left(t_0\right)_2\right]$ for intermediate values of $t-t_0$, and we display in Fig. 11 the comparison of the exact result and the approximation $c_\psi\left(t-t_0\right)$: beyond a certain value of $t-t_0$ the exact solution starts to deviate from the approximation c_ψ and approaches asymptotically the value $\frac{\Delta\phi_{\max}^2}{3}$. The approximation is rather accurate up to $t-t_0 \sim 2 \div 3 \times 10^4$ respectively for the Western and the Eastern grid.

F. Exponentials of the phase

Let us consider now the quantity

$$
x\left(t\right) \equiv \cos\left(\phi\left(t\right)\right) = \cos\left(\omega_c t + \psi\left(t\right)\right) \tag{74}
$$

which represent a model of the phase noise contribution to detector noise. It is convenient to rewrite x as

$$x(t) = \frac{1}{2}\left[z(t) + z^*(t)\right] \tag{75}$$

in terms of the complex process

$$z(t) \equiv e^{i[\omega_c t + \psi(t)]}. \tag{76}$$

We recall the useful identity

$$E\left[e^{\alpha\xi}\right] = e^{\alpha E[\xi] + \frac{1}{2}\alpha^2 E\left[(\xi - E[\xi])^2\right]} \tag{77}$$

valid for a gaussian variable ξ: applying to the case at hand, we obtain that

$$E[z(t)] = e^{i\omega_c t - \frac{1}{2}\sigma_\psi^2(t)} \tag{78}$$

and therefore

$$E[x(t)] = \cos(\omega_c t)\, e^{-\frac{1}{2}\sigma_\psi^2(t)}; \tag{79}$$

the process $x(t)$ is not stationary, although we can expect that the exponential is small for t large with respect to some epoch when the process has started. We are then interested in the covariance

$$C_{xx}(t+\tau, t) \equiv E\left[\left(x(t) - E[x(t)]\right)\left(x(t+\tau) - E[x(t+\tau)]\right)\right]; \tag{80}$$

it can be rewritten[2, pag. 369] in terms of the covariances of the variables z, z^* as follows

$$C_{xx}(t+\tau, t) = \frac{1}{2}\Re\left(C_{zz^*}(t+\tau, t) + C_{zz}(t+\tau, t)\right). \tag{81}$$

We obtain

$$\begin{aligned} C_{zz^*}(t+\tau, t) &= E\left[z(t+\tau)\, z^*(t)\right] - E\left[z(t+\tau)\right] E\left[z^*(t)\right] \\ &= e^{i\omega_c\tau}\left\{E\left[e^{i[\psi(t+\tau) - \psi(t)]}\right] - e^{-\frac{1}{2}E\left[\psi^2(t+\tau) + \psi^2(t)\right]}\right\} \\ &= e^{i\omega_c\tau}\left\{e^{-\frac{1}{2}c_\psi(\tau)} - e^{-\frac{1}{2}\left[\sigma_\psi^2(t+\tau) + \sigma_\psi^2(t)\right]}\right\} \end{aligned} \tag{82}$$

and

$$\begin{aligned} C_{zz}(t+\tau, t) &= E\left[z(t+\tau)\, z(t)\right] - E\left[z(t+\tau)\right] E\left[z(t)\right] \\ &= e^{i\omega_c(2t+\tau)}\left\{E\left[e^{i[\psi(t+\tau) + \psi(t)]}\right] - e^{-\frac{1}{2}E\left[\psi^2(t+\tau) + \psi^2(t)\right]}\right\} \\ &= e^{i\omega_c(2t+\tau) - \frac{1}{2}\left[\sigma_\psi^2(t+\tau) + \sigma_\psi^2(t)\right]}\left\{e^{-E[\psi(t+\tau)\psi(t)]} - 1\right\} \\ &= e^{i\omega_c(2t+\tau) - \frac{1}{2}\left[\sigma_\psi^2(t+\tau) + \sigma_\psi^2(t)\right]}\left\{e^{-\sigma_\psi^2(t) - (2\pi)^2\sigma_\nu^2\tau_\nu^2\left(1 - e^{-\frac{\tau}{\tau_\nu}}\right)} - 1\right\} \end{aligned} \tag{83}$$

the result for C_{xx} is complicated, unless we can assume that $\sigma_{\psi}^{2}(t), \sigma_{\psi}^{2}(t+\tau)$ are large. In that case we have simply

$$C_{xx}(t+\tau\, t) \approx \frac{1}{2}\cos(\omega_c \tau)\, e^{-\frac{1}{2}c_{\psi}(\tau)} \tag{84}$$

and the process can be considered stationary. In this limit there is no difference between covariance and correlation (the expectation values $E[x(t)]$ are zero in the large σ_{ψ}^{2} limit) and we can simply write

$$R_{xx}(\tau) = \frac{1}{2}\cos[2\pi\nu_c\tau]\, e^{-(2\pi)^2\sigma_{\nu}^2\tau_{\nu}|\tau|\left[1-\frac{\tau_{\nu}}{|\tau|}\left(1-e^{-\frac{|\tau|}{\tau_{\nu}}}\right)\right]}.$$

Given the correlation function, it is possible to compute the spectrum

$$\begin{aligned} S_{xx}(\omega) &= \int_{-\infty}^{+\infty} R_{xx}(\tau)\, e^{-i\omega\tau} d\tau \\ &= 2\int_{0}^{+\infty} R_{xx}(\tau)\cos(\omega\tau)\, d\tau \end{aligned} \tag{85}$$

in closed form, obtaining

$$S_{x}(\omega) = \frac{\tau_{\nu}}{2} e^{\alpha_{\nu}} \Re\left[\alpha_{\nu}^{-i(\omega-\omega_c)\tau_{\nu}-\alpha_{\nu}} \gamma\left(\alpha_{\nu} + i(\omega-\omega_c)\tau_{\nu}, \alpha_{\nu}\right)\right] + \omega_c \to (-\omega_c) \tag{86}$$

where γ is one of the two incomplete gamma functions [4, Eq. 8.350.1], defined as

$$\gamma(a,x) = \int_{0}^{x} e^{-t} t^{a-1} dt \tag{87a}$$

$$\Gamma(a,x) = \int_{x}^{\infty} e^{-t} t^{a-1} dt\,. \tag{87b}$$

Substituting the values for σ_{ν} and τ_{ν} estimated in IV E, Eqs. 63, we obtain rather large values

$$\alpha_{\nu} \approx \left(920,\ 1.6\times 10^{6}\right) \tag{88}$$

respectively for the Western and Eastern grid, because of the quadratic dependence on τ_{ν} which in turn is quadratic in $\Delta\phi_{\max}$.

We display in Fig. 12 the spectrum for values $\omega \sim \omega_c$, obtained with the parameters α_{ν}, τ_{ν}pertinent to the two electrical grids, and we draw the attention of the reader on the long tails, almost *lorenzian*-like. This estimate is expected to be inaccurate for small values of $\omega - \omega_c$, corresponding to large values of τ, when the approximate form $c_{\psi}(\tau)$ for the structure function is known to deviate from the correct one. We estimate from Fig. 11 that

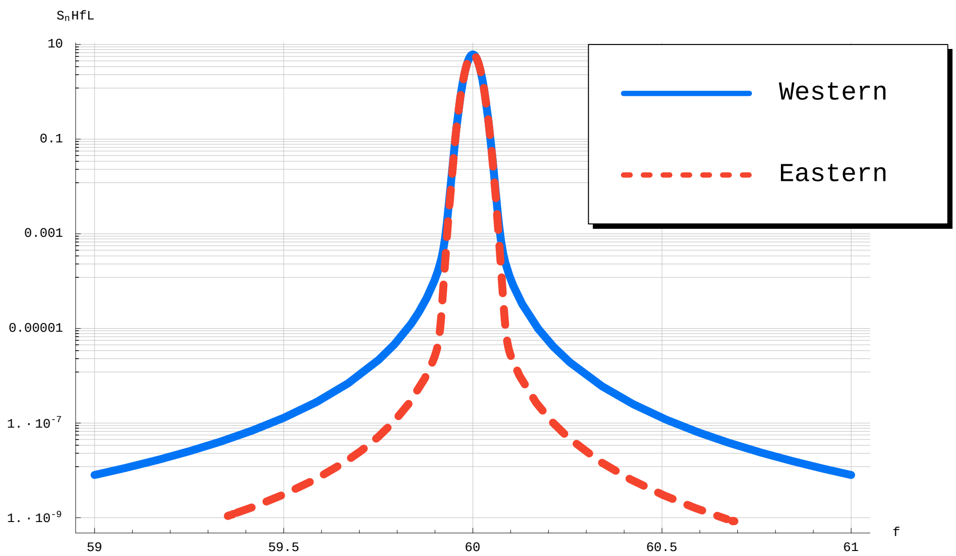

Figure 12: The line-shape at $\omega \sim \omega_c$ computed with the values of α_ν and τ_ν corresponding to the Western and Eastern grids. Corrections are expected for $\omega - \omega_c \leq \frac{1}{\tau_\nu \Delta\phi_{\max}} = (x, y)$

the deviations occur at values $\tau \geq 2 \div 3 \times 10^4$ respectively for the Western and Eastern grid, and correspondingly we surmise that the line-shape is not accurate for $(\nu - \nu_c) \leq 50 \div 33\,\mu$Hz.

We notice for completeness that if it were $\alpha_\nu \ll 1$, one might exploit the continued fraction expansion [7]

$$\gamma(a, x) = \frac{e^{-x} x^a}{a - \frac{ax}{a+x+1-\frac{(a+1)x}{a+x+2-\frac{(a+2)x}{a+x+3-\ldots}}}} \tag{89}$$

obtaining at second order

$$S_x(\omega) \approx \frac{\alpha_\nu \tau_\nu}{2} \left[\frac{(1+\alpha_\nu)(1+2\alpha_\nu)}{\left((\omega-\omega_c)^2 \tau_\nu^2 + \alpha_\nu^2\right)\left((\omega-\omega_c)^2 \tau_\nu^2 + (\alpha_\nu+1)^2\right)} + (\omega_c \to -\omega_c) \right]; \tag{90}$$

this approximation is reasonably good for values of α_ν up to ~ 1, but cannot be adopted for the large values appropriate in our case. At first order one would obtain a *lorenzian* curve.

G. Cross correlation among detectors

We are now interested in the cross-correlation of variables x_1, x_2

$$x_l(t) = \cos(\phi_l(t)) = \cos(\omega_c t + \psi_l(t)) \tag{91}$$

where the random phases ϕ_1, ϕ_2 are driven by frequencies ν_1, ν_2

$$\nu_l(t) = \nu_c + \delta\nu_l(t)\,. \tag{92}$$

both fluctuating around ν_c, and without loss of generality we have assumed that for both processes

$$E\left[\phi_l\left(t\right)\right] = \omega_c t; \tag{93}$$

one might want to introduce a constant phase difference, but it would only complicate the treatment. We assume to be able to measure the auto-correlations

$$\rho_{ll}\left(\tau\right) = E\left[\delta\nu_l\left(t+\tau\right)\delta\nu_l\left(t\right)\right] \tag{94}$$

and the cross-correlation

$$\rho_{12} \equiv E\left[\delta\nu_1\left(t+\tau\right)\delta\nu_2\left(t\right)\right]. \tag{95}$$

The distribution of the random variables $\boldsymbol{\delta\nu_1}, \boldsymbol{\delta\nu_2}$ shall be assumed Gaussian, hence in analogy with Eq. (43) we obtain

$$P\left(\boldsymbol{\delta\nu_1}, \boldsymbol{\delta\nu_2}\right) \propto \exp\left[-\frac{1}{2}\int_{-\infty}^{+\infty}\left(\delta\tilde{\nu}_1\left(\omega\right), \delta\tilde{\nu}_2\left(\omega\right)\right)^* \left[\mathsf{S}\left(\omega\right)\right]^{-1}\begin{pmatrix}\delta\tilde{\nu}_1\left(\omega\right)\\ \delta\tilde{\nu}_2\left(\omega\right)\end{pmatrix}\frac{d\omega}{2\pi}\right] \tag{96a}$$

$$\mathsf{S}\left(\omega\right) \equiv \begin{pmatrix} S_{\nu_1\nu_1}\left(\omega\right) & S_{\nu_1\nu_2}\left(\omega\right)\\ S^*_{\nu_1\nu_2}\left(\omega\right) & S_{\nu_2\nu_2}\left(\omega\right)\end{pmatrix} \tag{96b}$$

where the relations

$$S_{\nu_k\nu_l}\left(\omega\right) = \int_{-\infty}^{+\infty}\rho_{kl}\left(\tau\right)e^{-i\omega\tau}d\tau \tag{97}$$

hold.

We can assume again an exponential form for the autocorrelations

$$\rho_{ll}\left(\tau\right) = \sigma^2_{\nu_l}e^{-\frac{|\tau|}{\tau_{ll}}} \tag{98}$$

but we have no model for the cross correlation $\rho_{12}(\tau)$, which might also be identically zero if the two power grids are totally unrelated. From the identity

$$\rho_{11}\left(0\right) + \rho_{22}\left(0\right) - 2\rho_{12}\left(\tau\right) = E\left[\left(\delta\nu_1\left(t+\tau\right) - \delta\nu_2\left(t\right)\right)^2\right] \tag{99}$$

one can deduce the inequality

$$\rho_{12}\left(\tau\right) \leq \frac{1}{2}\left(\rho_{11}\left(0\right) + \rho_{22}\left(0\right)\right) \tag{100}$$

which is not very stringent. We are interested in both the cross-correlation

$$R_{x_1x_2}\left(t+\tau, t\right) \equiv E\left[x_1\left(t+\tau\right)x_2\left(t\right)\right] \tag{101}$$

and the cross-covariance

$$C_{x_1x_2}(t+\tau,t) \equiv E\left[\left(x_1(t+\tau)-E\left[x_1(t+\tau)\right]\right)\left(x_2(t)-E\left[x_2(t)\right]\right)\right]$$
$$= E\left[x_1(t+\tau)\,x_2(t)\right]-E\left[x_1(t+\tau)\right]E\left[x_2(t)\right]. \qquad (102)$$

Again we introduce the complex quantities

$$z_k(t)=e^{i\omega_c t}e^{i\psi_k(t)} \qquad (103)$$

which enable us to write the cross correlation as

$$C_{x_1x_2}(t+\tau,t)=\frac{1}{2}\Re\left[C_{z_1z_2^*}(t+\tau,t)+C_{z_1z_2}(t+\tau,t)\right]. \qquad (104)$$

Following the discussion made in the single detector case we might be tempted to neglect the expectation values

$$E\left[z_k(t)\right]=e^{i\omega_c t}e^{-\frac{1}{2}\sigma^2_{\psi_k}(t)} \qquad (105)$$

and surmise that $C_{x_1x_2}\sim R_{x_1x_2}$: let us resist, proceeding to calculate each of the terms. We have that

$$C_{z_1z_2^*}(t+\tau,t)=R_{z_1z_2^*}(t+\tau,t)-e^{i\omega_c\tau}e^{-\frac{1}{2}\left[\sigma^2_{\psi_1}(t+\tau)+\sigma^2_{\psi_2}(t)\right]} \qquad (106)$$

and in turn

$$\begin{aligned} R_{z_1z_2^*}(t,t+\tau) &\equiv E\left[z_1(t+\tau)\,z_2^*(t)\right] \\ &= e^{i\omega_c\tau}E\left[e^{i(\psi_1(t+\tau)-\psi_2(t))}\right] \\ &= e^{i\omega_c\tau}e^{-\frac{1}{2}E\left[(\psi_1(t+\tau)-\psi_2(t))^2\right]} \end{aligned} \qquad (107)$$

hence

$$C_{z_1z_2^*}(t+\tau,t)=e^{i\omega_c\tau}e^{-\frac{1}{2}\left[\sigma^2_{\psi_1}(t+\tau)+\sigma^2_{\psi_2}(t)\right]}\left\{e^{E[\psi_1(t+\tau)\psi_2(t)]}-1\right\} \qquad (108)$$

and analogously

$$C_{z_1z_2}(t+\tau,t)=e^{i\omega_c(2t+\tau)}e^{-\frac{1}{2}\left[\sigma^2_{\psi_1}(t+\tau)+\sigma^2_{\psi_2}(t)\right]}\left\{e^{-E[\psi_1(t+\tau)\psi_2(t)]}-1\right\}. \qquad (109)$$

The above expressions show that we cannot let $\sigma^2_{\psi_l}\to 0$, because we would cancel any effect. We notice that *if* $E\left[\psi_1(t+\tau)\,\psi_2(t)\right]=0$, that is *if* the processes $\boldsymbol{\psi_{1,2}}$are uncorrelated, the cross-covariance $C_{x_1x_2}$ results identically zero, while the cross-correlation is

$$R_{x_1x_2}(t+\tau,t)=\cos\left(\omega_c(t+\tau)\right)\cos\left(\omega_c t\right)e^{-\frac{1}{2}\left[\sigma^2_{\psi_1}(t+\tau)+\sigma^2_{\psi_2}(t)\right]}. \qquad (110)$$

At the other extremum, if the two processes were perfectly correlated or anti-correlated, for instance

$$\psi_1(t) = \psi_2(t) \quad \text{or} \quad \psi_1(t) = -\psi_2(t)\,, \tag{111}$$

one would have a not zero result, exactly equal to the one considered in the single detector case, dominated respectively by $C_{z_1 z_2^*}$ or $C_{z_1 z_2}$.

The general case lies in between: recall that we have proven in Eq. (61) that the variances $\sigma^2_{\psi_l}(t)$ are not-decreasing functions of t: this means that proceeding backwards in time there exist a time t_0 at which the variance of one of the processes was zero. We shall therefore make the *ansatz* that a epoch t_0 exists at which *both* the variances can be assumed zero and that $\psi_1(t_0), \psi_2(t_0)$ can be assumed to be zero. We shall discuss later what is the dependence of the results on the value of t_0, whose statistics is not known to us: for simplicity we shall set $t_0 = 0$, but keeping in mind that we have assumed a special role for that epoch: in particular this choice means that

$$\sigma^2_{\psi_i}(t) = \alpha_i \left(\frac{t}{\tau_i}\right) \tag{112}$$

where

$$\alpha_i \equiv 2\left(2\pi\sigma_{\nu_i}\tau_{\nu_i}\right)^2. \tag{113}$$

Averaging the cross correlation of the $\boldsymbol{\psi_1, \psi_2}$ processes over the frequency noise, we obtain

$$\begin{aligned} E_{\boldsymbol{\delta\nu}}\left[\psi_1(t+\tau)\,\psi_2(t)\right] &= E\left[\left(\psi_1(t+\tau) - \psi_1(0)\right)\left(\psi_2(t) - \psi_2(0)\right)\right] \\ &= (2\pi)^2 \int_0^{t+\tau} d\tau_1 \int_0^t d\tau_2 E_{\boldsymbol{\delta\nu}}\left[\delta\nu_1(t+\tau)\,\delta\nu_2(t)\right] \\ &= (2\pi)^2 \int_0^{t+\tau} d\tau_1 \int_0^t \rho_{\nu_1\nu_2}(\tau) \\ &= (2\pi)^2 \int_{-\infty}^{+\infty} \frac{d\omega}{2\pi}\frac{1}{\omega^2}\left[1 + e^{i\omega\tau} - e^{-i\omega t} - e^{-i\omega(t+\tau)}\right] S_{\nu_1\nu_2}(\omega)\,; \end{aligned} \tag{114}$$

next we assume that $\rho_{\nu_1\nu_2}$ is even in τ, and therefore $S_{\nu_1\nu_2}$ is real, hence

$$E_{\boldsymbol{\delta\nu}}\left[\psi_1(t+\tau)\,\psi_2(t)\right] = (2\pi)^2 \int_{-\infty}^{+\infty} \frac{d\omega}{2\pi}\frac{2}{\omega^2}\left[\sin^2\left(\frac{\omega t}{2}\right) + \sin^2\left(\frac{\omega(t+\tau)}{2}\right) - \sin^2\left(\frac{\omega\tau}{2}\right)\right] S_{\nu_1\nu_2}(\omega)\,. \tag{115}$$

Finally if we assume an exponential correlation

$$\rho_{12}(\tau) = \sigma^2_{12} e^{-\frac{|\tau|}{\tau_{12}}} \tag{116}$$

where σ_{12}^2 can be negative. We obtain the lorenzian cross-spectrum

$$S_{\nu_1\nu_2}(\omega) = \frac{2\sigma_{12}^2\tau_{12}}{1+(\omega\tau_{12})^2} \tag{117}$$

and

$$\begin{aligned} E\left[\psi_1(t+\tau)\,\psi_2(t)\right] &= \frac{1}{2}\alpha_{12}\left[\frac{|t+\tau|+|t|-2|\tau|}{\tau_{12}}\right. \\ &\qquad\left. +\left(e^{-\frac{|t+\tau|}{\tau_{12}}}+e^{-\frac{|t|}{\tau_{12}}}-e^{-\frac{|\tau|}{\tau_{12}}}-1\right)\right]. \end{aligned} \tag{118}$$

where

$$\alpha_{12} \equiv 2(2\pi)^2\sigma_{12}^2\tau_{12}^2. \tag{119}$$

Assembling the results we have

$$\begin{aligned} R_{x_1x_2}(t+\tau\, t) &= \frac{1}{2}\cos(\omega_c(2t+\tau))\, e^{-\frac{1}{2}\left(\alpha_1\frac{t+\tau}{\tau_1}+\alpha_2\frac{t}{\tau_2}\right)-E[\psi_1(t+\tau)\psi_2(t)]} \\ &+ \frac{1}{2}\cos(\omega_c t)\, e^{-\frac{1}{2}\left(\alpha_1\frac{t+\tau}{\tau_1}+\alpha_2\frac{t}{\tau_2}\right)+E[\psi_1(t+\tau)\psi_2(t)]} \end{aligned} \tag{120}$$

where we understand that the expression is valid only for both $t+\tau>0$ and $t>0$, because of the special meaning of the $t=0$ epoch. The explicit dependence on t means that it is strictly speaking not possible to define the spectrum. We can define a time-dependent approximate cross-spectrum

$$S_{12}(\omega,t) = \int_{-T}^{+T} R_{x_1x_2}(t+\tau,t)\,d\tau \tag{121}$$

where we should limit $T \le t$.

V. SUMMARY

The observed long-term correlations in the mains are consistent with what we have learned on how frequency stabilization is imposed on the U.S. power grid by the authorities of the two regions. The common use of GPS guarantees that some level of coherence will be present. The single-sided power spectral density will exhibit sideband structure up to a scale of m̃Hz.

The data we obtained are for the Western U.S. region only and so at this point it is not possible to determine the cross-correlation function $\rho_{12}(\tau)$. This is a work in progress and as more information becomes available, this document will be updated.

Appendix A: REFERENCE FORMULAS

We list here our conventions for the Fourier transforms and some other useful identities

1. Fourier transform conventions

We follow the conventions adopted in [2, 3]. If $x \leftrightarrow \tilde{x}$ are a Fourier transform pair, and i is the imaginary unit, we have

$$x(t) = \int_{-\infty}^{+\infty} e^{i\omega t} \tilde{x}(\omega) \frac{d\omega}{2\pi} \tag{A1a}$$

$$\tilde{x}(\omega) = \int_{-\infty}^{+\infty} e^{-i\omega\tau} x(\tau)\, d\tau \tag{A1b}$$

which correspond, in the discrete time, discrete frequency case, to

$$x[l] = \frac{1}{dt\, N} \sum_{k=0}^{N-1} e^{i2\pi kl/N} \tilde{x}[k] \tag{A2a}$$

$$\tilde{x}(\omega) = dt \sum_{l=0}^{N-1} e^{-i2\pi kl/N} x[l] \tag{A2b}$$

where dt is the sampling interval ($1/(2\,dt)$ is the Nyquist frequency) and N is the number of samples, corresponding to a observation time $T = N\,dt$.

2. Useful identities

Recall that if the distribution of x is

$$P(\boldsymbol{x}) = \mathcal{N} e^{-\frac{1}{2}\int\int \frac{d\tilde{x}(\omega)}{2\pi} \frac{2\pi\delta\left(\omega-\omega'\right)}{S_x(\omega)} \frac{d\tilde{x}^*(\omega')}{2\pi}} \tag{A3}$$

the functional integral

$$\int \mathrm{D}\left(\mathrm{d}\tilde{\mathrm{x}}\right) P(\boldsymbol{x})\, e^{ip\int e^{i\omega t} d\tilde{x}(\omega)} \tag{A4}$$

is a usual Gaussian integral and we obtain

$$E\left[e^{ipx(t)}\right] = e^{-\frac{1}{2}p^2 \int S_x(\omega) \frac{d\omega}{2\pi}} \tag{A5}$$

which is just a particular case of the general expression

$$E\left[e^{i\int_{-\infty}^{+\infty} x(\tau)s(\tau)d\tau}\right] = e^{-\frac{1}{2}\int |\tilde{s}(\omega)|^2 S_x(\omega) \frac{d\omega}{2\pi}}\ ; \tag{A6}$$

for the generating function of the correlations of the $x\left(t\right)$ variables, in terms of the source s. The last relation is very handy: for instance, setting $s\left(\tau\right)=p\,\delta\left(\tau-t\right)-p'\delta\left(\tau-t'\right)$ one easily obtains

$$\begin{aligned}E\left[e^{i(px(t)-qx(t'))}\right] &= e^{-\frac{1}{2}\int\left[(p-q)^2+4pq\left(\sin\left(\frac{\omega(t-t')}{2}\right)\right)^2\right]S_x(\omega)\frac{d\omega}{2\pi}} \\ &= e^{-\frac{1}{2}\left[\left(p^2+q^2\right)R_x(0)-2pqR_x(t-t')\right]}\end{aligned} \tag{A7}$$

in terms of the correlation function $R_x\left(\tau\right)\equiv\int S_x\left(\omega\right)e^{i\omega\tau}\frac{d\omega}{2\pi}$.

[1] Information obtained by phone from the U.S. western grid authority.

[2] A.Papoulis, *Probability, random variables, and stochastic processes*, (McGraw-Hill, New York, 1991).

[3] D.B.Percival and A.T.Walden, *Spectral analysis for physical applications*, (Cambridge Univ. Press, Cambridge, 1993).

[4] I.S.Gradshteyn and I.M.Ryzhik, *Table of integrals, series and products*, (Academic Press, New York, 1965).

[5] A.M.Yaglom, *An introduction to the theory of stationary random functions*, (Prentice-Hall, Englewood Cliffs, 1962).

[6] J.L.Doob, *Stochastic processes*, (John Wiley & Sons, New York, 1953).

[7] Wolfram Research Inc, http://functions.wolfram.com/06.07.10.0003, (2001).

[8] A.M.Sintes and B.F.Schutz, Phys.Rev.D**58**, 122003 (1998).

[9] A.M.Sintes and B.F.Schutz, Phys.Rev.D**60**, 062001 (1999).

[10] B.Allen and J.D.Romano, Phys. Rev. D**59**, 102001 (1999).